Optimizing the preheating temperature of hot rolled slab from the perspective of the oxidation kinetic

Zhang, Hua; Yu, Li; Liu, Tao; Ni, Hongwei; Li, Yang; Chen, Zhiyuan; Yang, Yongxiang

Important note
To cite this publication, please use the final published version (if applicable).
Please check the document version above.

Original Article

Optimizing the preheating temperature of hot rolled slab from the perspective of the oxidation kinetic

Hua Zhang [a], Li Yu [a], Tao Liu [a], Hongwei Ni [a], Yang Li [a,c,*], Zhiyuan Chen [b,c,*], Yongxiang Yang [c]

[a] _The State Key Laboratory of Refractories and Metallurgy, Key Laboratory for Ferrous Metallurgy and Resources Utilization of Ministry of Education, Wuhan University of Science and Technology, Wuhan 430081, China_
[b] _Separation and Conversion Technology, Flemish Institute for Technological Research (VITO), Boeretang 200, Mol 2400, Belgium_
[c] _Department of Materials Science and Engineering, Technische Universiteit Delft, 2628 CD, Delft, The Netherlands_

ARTICLE INFO

ABSTRACT

Decreasing the preheating temperature is an effective step to control the energy consumption in the hot rolling process. In order to obtain the lowest preheating temperature to prepare enough thickness of oxide scale in the hot rolling process, the oxidation resistance of commercial steel samples with different Al and Si contents were investigated in this paper. The results indicate that both Al and Si based oxides form at the steel-oxides interface as diffusion barrier but Al provide stronger diffusion resistance than Si in the diffusion-controlling oxidation region. Meanwhile, a three-dimensional oxidation kinetic model has been adopted to depict the oxidation behavior of four types of commercial steel. The oxidation process of automotive steel sample containing with low alloy elements is kinetically determined by interface chemical reaction. Its activation energy is 55.2 ± 6.9 kJ/mol. As for silicon steel containing with relative high alloy elements, its controlling process is determined by diffusion step at low temperature and controlled by chemical reaction rate at high temperature. In order to obtain enough thickness of oxide scale, the lowest preheating temperature of different types steel range from high to low should be the steel with high content of Al (1180 °C), the steel with high content of Si and low content of Al (1130 °C) and the steel with high contents of Si and Al (1030 °C).

1. Introduction

Hot rolling plays a very important role in manufacturing bulk products in the flat metal manufacture. The hot rolling process consists of furnace heating, primary descaling, roughing mills, secondary descaling, finishing mills, run out table and coiling processes [1]. In furnace heating process, the work-piece is heated to sufficiently high temperatures to reduce its strength. Meanwhile, it should be noted that the slab is exposed in oxidizing atmosphere at high temperatures after the heating process. In this period, the heated slab can react with oxygen and water, resulting in a thermal oxide scale covered the metal surface. The oxide scale is typically composed of three layers: hematite (Fe_2O_3) at the outer surface, magnetite (Fe_3O_4) at the intermediate region, and wüstite (FeO) at the inner region close to the interface [1,2]. This three-layer structure is not stable because the oxidation or substrate stress at the lower temperatures in cooling stage, which induces the structures transformation of oxide scale at different parts of the strip. In the following descaling and mill process, some defects on the surface of slab can be removed with the oxide scale, which is beneficial to improve the surface quality of the obtained slab [3,4]. Hence, it is an important issue to investigate the influence factors on the formation of the thermal oxide scale in the hot-rolling process.

According to the literature [1,5–9], it is known that the cooling rate, heat-treatment temperature, exposure time and composition of steel substrate are the major factors influencing the growth and structure of the oxide scale. The influence of these factors on the evolutions of oxide scale has been investigated intensively in recent years. Yearian et al. [10] and Taniguchi et al. [11] investigated the effect of oxidation temperature on the formed oxide scales at $700-1160\,^{\circ}C$. The results showed that the oxidation rates increased with the increasing of oxidation temperature. Meanwhile, some alloy elements such as Cr or Si would react with FeO layer to form Fe_2SiO_4 or $FeCrO_4$, which can change the porosity of obtained oxide scales. Suarez et al. [12] also found that the addition of alloying elements has an important impact on scale properties. In particular the alloying of silicon effects the region between scale and substrate obviously. Fukagawa et al. [13,14] used Si-added steel with different contents of Si to study the formation mechanism of oxide scale in hot rolling process. They found that the composition of oxide scale formed in different rolling step varied obviously. It gives a guidance to prevent scale defects in Si-added steels in real production. Cheng et al. [15] investigated the high-temperature oxidation behavior of aluminide steel with silicon contents varying from 0% to 5 wt.%. The results indicate that the addition of silicon would change the microstructure and phase constitution of aluminide steel, which further affected its isothermal and cyclic oxidation resistance abilities at high temperature. The isothermal oxidation rates of the aluminide steel increased as the silicon content in the aluminum layers increased. Alaoui [16], Liu [17] and Yuan [18] et al. investigated the effect of silicon contents on the oxidation process of silicon-containing steels. The results indicate that the silicon would delay scale growth by forming a silica barrier layer at the interface. Meanwhile, a fayalite-wüstite eutectic would be formed when the

oxidation temperature is higher than $1177\,^{\circ}C$. This molten phase favors iron diffusion leading to fast scale growth. However, these research mainly used synthetic steel to investigate the oxidation process. The synergic influence of Si and Al on the commercial steel is not clear.

Due to the cruel market competition and rigorous control of energy consumption, more and more factories desire to obtain high quality slab with lower preheating temperature. However, it will lead to the thin oxide scale, which discourages the removal of the surface defect and further impede the improvement of slab surface quality. The aforementioned literatures showed that even a little difference of track elements in the slab substrate has significant influence on the property of the oxide scale formed during the hot rolling process. These oxide scales further have effect on the surface microstructures and cracks of the obtained slab [19]. Hence, it is necessary to discover the role of the common elements such as Si and Al in different steel played on the formation of oxide scale during the hot rolling process. Especially, the relationship between the element contents in steel matrix and the formation mechanism of the oxide scales should be investigated systematically. In this paper, the growth of oxide scale on the surface of four typical steels with different contents of common alloying elements were investigated. Our attention was focused on Si and Al to illustrate the effect of the contents of these elements on the thickness of scale formation. We established a kinetic model to analyze the oxidation process and derived an equation to explain the growth rate of scale with different control steps. The analysis result should be beneficial for the controlling of the preheating temperature in the hot rolling process aim to different steel, improving the quality of the hot rolled slab and decreasing the cost of the production.

2. Experimental

Four types of steels (containing silicon steel and automotive steel) were investigated in this study, of which the chemical compositions are listed in Table 1. The principal differences of these samples are the contents of Si and Al. As for 30Q140, it is an oriented silicon steel and representative steel with high content of Si and low content of Al. 50WW800 and 50WW470 are non-oriented silicon steel, they are representative steels with high content of Al and different contents of Si, respectively. As for DX51D + Z, it is automotive steel with low contents of Si and Al.

The isothermal oxidation experiments of these steel samples were carried out on a simultaneous thermal analysis (Netsch, STA449C) with a nominal sensitivity of $0.1\,\mu g$. The samples were machined into pieces with dimensions of $4\,mm \times 4\,mm \times 5\,mm$, and then polished with a series of emery papers up to 1500 grit. After polishing, the samples were ultrasonicated in ethanol for 10 min to remove the residual on the surface. The degreased samples were loaded into the Al_2O_3 crucible and heated to the assigned temperature by the heating rate of $10\,^{\circ}C/min$ in argon atmosphere. Then, compressed dry air was purged into the reactor with gas flow rate at 50 mL/min for oxidation reaction when the temperature reached preset temperature. The oxidation reaction

Table 1 – Chemical composition of the steel samples.

Tag[a]	30Q140	50WW800	50WW470	DX51D + Z
C	0.025−0.04	≤0.0030	≤0.0030	0.020−0.060
Si	3.10−3.2	1.80−2.20	0.25−0.70	≤0.040
Mn	0.15−0.2	0.15−0.35	0.30−0.70	0.10−0.40
P	≤0.02	≤0.030	0.050−0.110	≤0.020
S	≤0.015	≤0.0060	≤0.008	≤0.020
Al	0.010−0.025	0.20−0.40	0.25−0.50	0.020−0.060
N	0.0085−0.0115	≤0.0040	≤0.0050	≤0.0060
As	≤0.020	≤0.020	≤0.020	–

[a] 30Q140 is typical steel with high content of Si and low content of Al; 50WW800 is typical steel with high content of Si and Al; 50WW470 is typical steel with low content of Si and high content of Al; DX51D + Z is typical steel with high content of Si and Al.

lasted for 120 min. During the oxidation reaction, the reacting temperatures are controlled at 930, 1030, 1130, 1180, 1230 °C, respectively. The samples were cooled down in the reactor under the protection of argon gas after the oxidation.

The oxidized samples were mounted in resin and polished to exposure the cross sections for following characterization. A field emission scanning electron microscope (SEM) with energy dispersive spectrometer (EDS) as attachment (FESEM, FEI Nova 400 Nano) is employed for the microstructure characterization.

3. Results and discussions

3.1. Thickness of the oxides scale

Fig. 1 shows the cross sections of the oxidized samples at 930 °C for 120 min. Al and Si are well-known as the alloying elements to retard the high-temperature oxidation process of steel [20]. The high affinity of Al and Si for oxygen results in a formation of Al and Si based oxides. They have the potential to form dense oxide film or network to decrease the diffusion rate of ions. Because of the relatively high concentration of the alloy elements Si and Al in the steels except for DX51D + Z, the oxides scale on the samples are within 10 μm. The low content of Si and Al contributes the relatively serious oxidation of DX51D + Z steel. An empirical relationship between Si + Al content in the steel and the thickness of the oxides scale is suggested as following:

$$\log_{10}[y(\mu m)] = (1.56 \pm 0.08)\text{-}(0.16 \pm 0.03)\text{Si[wt\%]}$$

$$\text{-}(2.28 \pm 0.25)\text{Al[wt\%]} \tag{1}$$

where, y is the thickness of the oxides scale. The Eq. (1) implies that there is no synergistic effect between Si and Al to inhibit oxidation. The relationship between the thickness of oxide scale and the contents of Al and Si is shown in Fig. 2a, which is drew by fitting the values obtained from Eq. (1). Fig. 2b depicted the thickness of the oxide scale obtained in different commercial steels. According to the contents of Al and Si in these steels, the estimated values of the oxide scales can be calculated according to Eq. (1) or Fig. 2a. It can be seen that the fitted value distributed in the range of the measured values, indicating that the equation can predict the thickness of the obtained oxide scale accurately. Although it was reported in other alloys with both Al and Si additions in either positive

or negative effects [21,22]. It can be the reason that the Al content is too low to interact with the SiO$_2$ formation. Usually, Si is selectively oxidized at the interface between oxides scale and steel matrix. It was reported that 1 wt.% of silicon in the Austenitic alloy formed SiO$_2$ or Fe$_2$SiO$_4$ particles under the oxides scale [12]. These particles could decrease the oxidation rate of the alloy by 50-400%. When the silicon content was increased to 4 wt.% in the alloy, a sub layer contains SiO$_2$ or Fe$_2$SiO$_4$ could form, which can obviously supress the oxidation of alloy as a diffusive barrier [23]. Dunning et al. [21] indicated another mechanism that Si oxide forms networks at the grain boundaries under the oxides scale, which retard the outward diffusion of cations. The study of Martínez-Cázares et al. [24] also indicated that silicon in low content only forms islands of Fe$_2$SiO$_4$ at the oxide-steel interface, which can only provide limited resistance to the diffusion of ions across the oxides scale. Moreover, comparing to Si, Al acted stronger to protect the steels from oxidation in the current work. There are several proposed mechanisms for the effect of Al on the oxidation resistance of steel. Al forms discrete Al$_2$O$_3$ particles in the metallic matrix of chromium alloys [21]. A small amount of FeAl$_2$O$_4$ spinel was investigated in the low alloy steel at the hot rolling temperature. It can promote the oxides scale adherence on the metallic matrix [25]. It is also indicated that Al can increase the formation temperature of wustite, in which the outward diffusion of iron cations is faster than them in magnetite [26].

It is noted from Fig. 1 that, with the increasing of the thickness of the oxides scale, the physical contact between the steel matrix and the oxides scale becomes poor. It is well-known that the molar volumes of oxides and metal are different. The oxidation is comparing with a change in molar volume of the sample. It results in a tensile or compressive stress along the oxides scale in the oxidation. Thick oxides scale formed in 30Q140 and DX51D + Z steels can result in a high growth stress and residual stress of the scale in the oxidation and the cooling process, respectively [27,28]. The growth stress can modify the micro-structure and morphology of the oxides scale [29]. For instance, the gap between the oxides scale and the metallic matrix was the result of the high growth stress of the oxides scale on 30Q140 and DX51D + Z samples.

3.2. Compositions

The EDS analysis was employed to detect the chemical composition of the layers. Fig. 3 shows that the principal com-
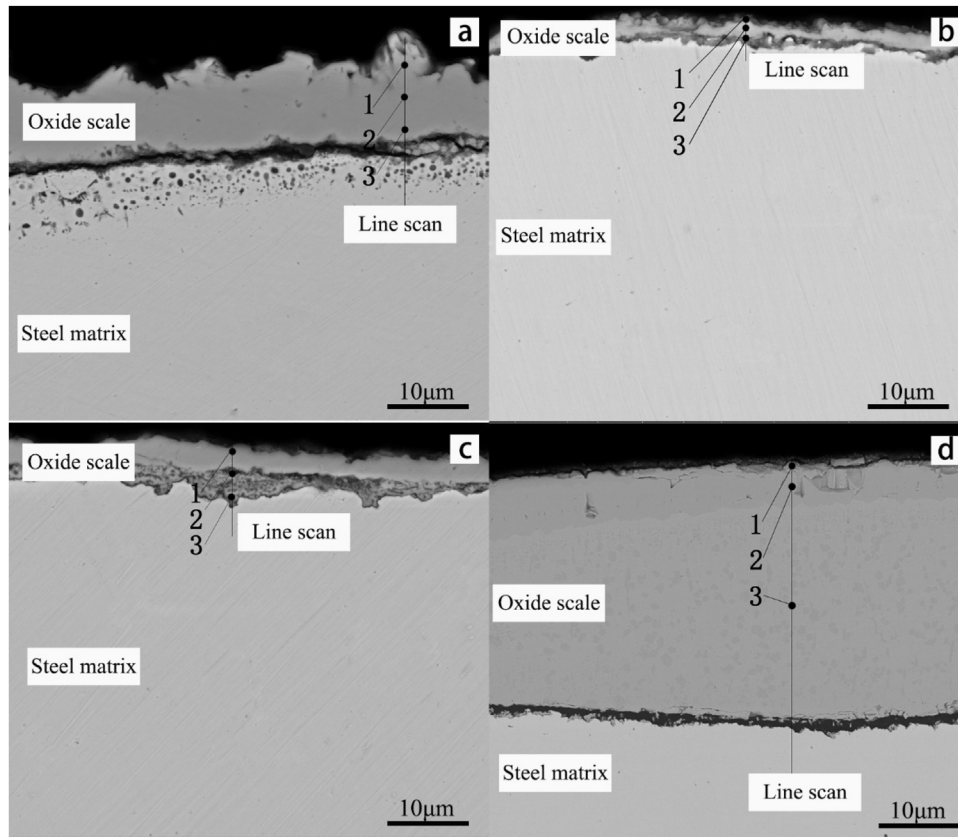
Fig. 1 – Cross sections of the oxidized samples: (a) 30Q140 ; (b) 50WW800; (c) 50WW470; (d) DX51D + Z.
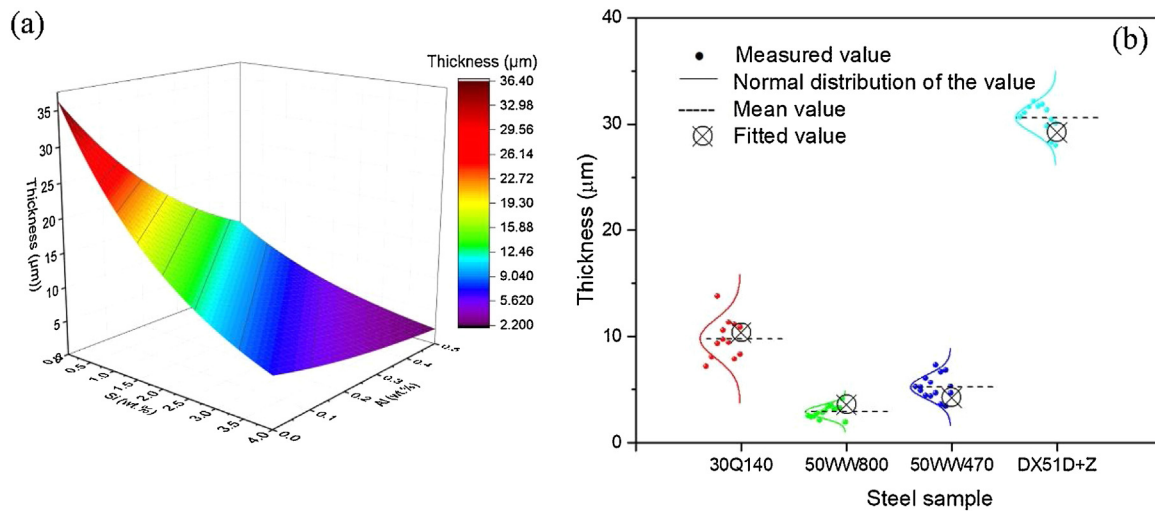

Fig. 2 – (a) The relationship between the thickness of oxide scale and the contents of Al and Si, (b) the thickness of the oxide scale in different commercial steels.

positions in the oxides scale are iron, silicon and aluminum. However, the silicon and aluminum contents in the steel are not high enough to form a protective oxide layer to protect the steel from further oxidation. Therefore, the out layer of the oxidized steel is iron oxides. There is only one layer of the oxides scale of the 30Q140 sample, but a serious internal oxidation is observed in its matrix. It resulted in a layer with a

porous matrix composed by loss and coarse steel grains. The EDS results of the corresponding cross sections are shown in Fig. 3(a). It implies that the reactions between the dissolved oxygen and the Si formed SiO_2 particles at the steel grain boundaries in this layer. Moreover, few Si was observed in the oxide scale. The high porosity of the metallic sub-layer is due to the Kirkendall effect of the diffusion of the ions [30]. Vacan-
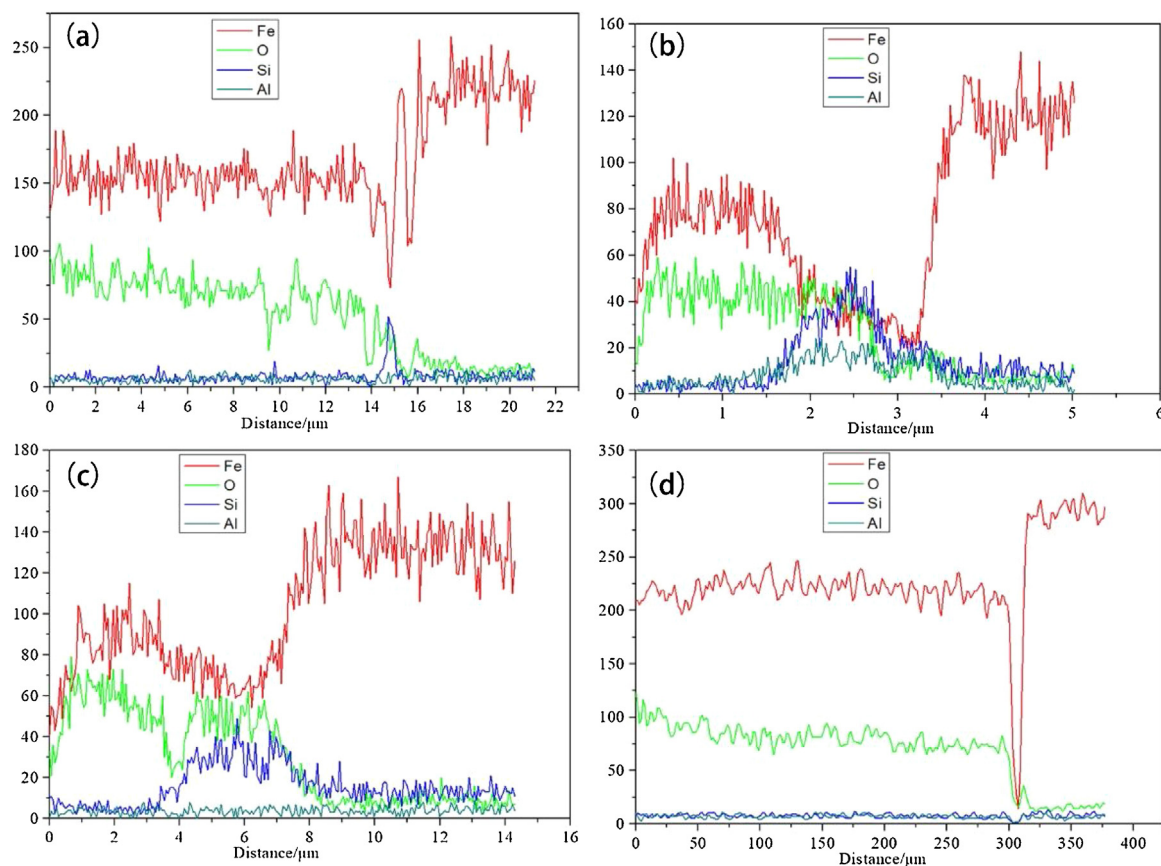
Fig. 3 – Chemical composition of the cross sections of the steels in Fig. 1. (a) 30Q140; (b) 50WW800; (c) 50WW470; (d) DX51D + Z.

cies were leaved in the matrix when the cations diffused out to form oxides scale to form these pores. The experimental results indicate that the Kirkendall effect is more serious at higher silicon content of the steel. The experimental results indicate that the Kirkendall effect is more serious at higher silicon content of the steel.

In addition, both the Al and Si contents in the oxides scale of 50WW800 are relatively high within the four samples. Correspondingly, 50WW800 showed the highest oxidation resistance in this work. The EDS analysis indicates that both Si and Al based compounds formed as under layer of the oxides scale. It is obvious that there are two layers of the oxides scale on the oxidized 50WW470 and DX51D + Z steel samples. However, the compositions are somehow different. A sub-layer is observed as silicon-rich oxides, in which Fe_2SiO_4 and SiO_2 can exist. Moreover, it is well known that even small amount of silicon additions in the steel can form silica adjacent to the metal, which increases the oxidation resistance of the steel. If a silica layer forms, it can be a diffusion barrier to retard the growth of the oxides scale [30].

3.3. Kinetics

Fig. 4 shows the mass gain curves of the four steels at different temperatures. The mass gains rates of the steel samples were relatively low at 930 °C except for D51D + Z steel. It keeps con-

stant with the SEM observation results, that the relatively high content of Si and Al can retard the oxidation process. At lower temperatures for most of the steel samples, the mass gains keep at a relatively low values (< 20 mg/cm²), and the curves are parabolic-like, indicating that the scale can provide a certain oxidation resistance. Meanwhile, the rate-determining step of the oxidation could be diffusion of ions in the oxides scale. It means that the oxidation is fast at the beginning. The very initial oxidation rate is infinite according to the kinetic models. And then the oxidation rate is limited at a low level with the slowly growing of dense oxides scale. However, it can be predicted that the oxidation process of a steel sample would not always follow the same kinetic mechanism with the extending exposure time. The previous research report [31] showed that there were three oxidation stages in the oxidation process of Fe-16Cr alloy. Therefore, this diffusion controlling oxidation may turn to be a break-away oxidation after a certain time.

Not only time but also temperature changes the oxidation kinetic mechanism. The positive effect of the alloy elements on the oxidation resistance is weaker at high temperature. All the steel samples showed break-away oxidation at higher temperatures (from 1030 °C). The accelerated oxidation rate of the steel sample implies that the main composition of the oxides scale is iron oxides, and the structure of it is should be coarse and loss. It can be noted that the mass gain curves are not
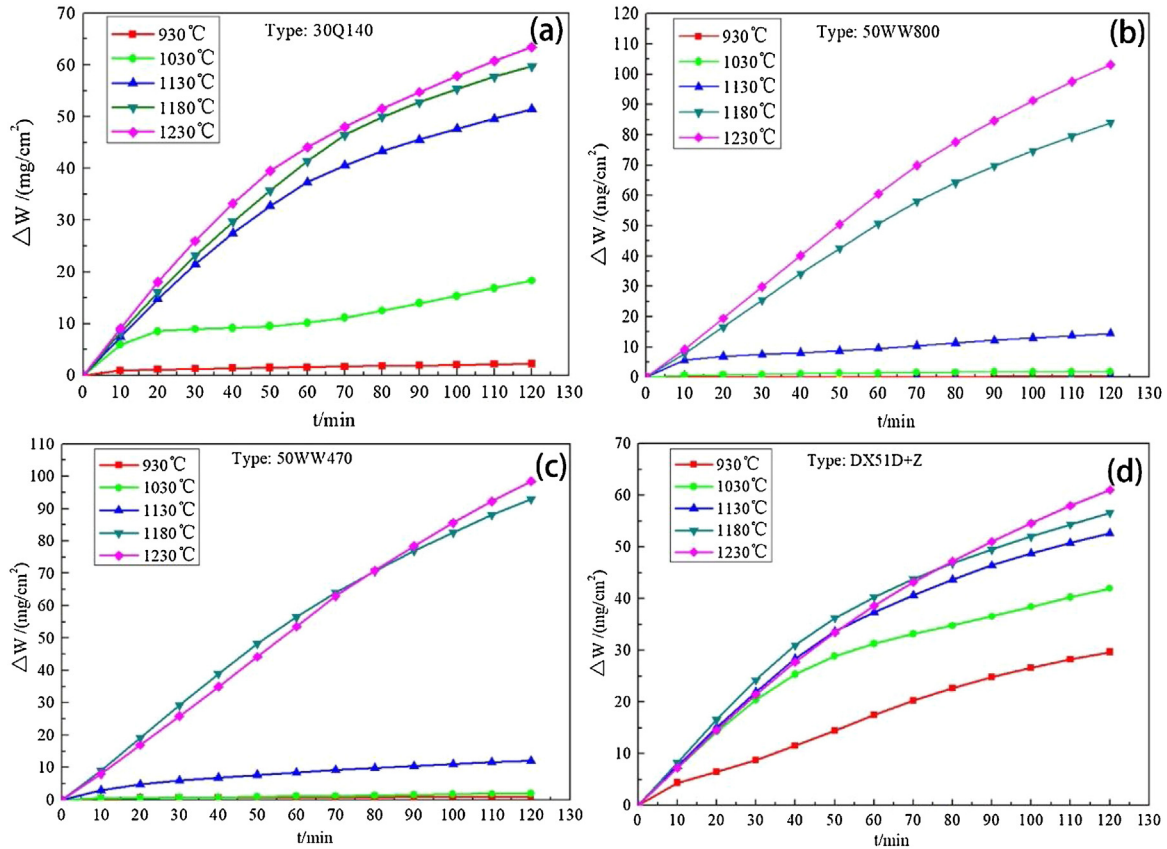
Fig. 4 – Mass gain of (a) 30Q140; (b) 50WW800; (c) 40WW470; (d) DX51D + Z steels in air atmosphere at different temperatures, where the curves are the fitting results.

parabolic, where the rate-determining step of the oxidation turns to be an interfacial chemical reaction [31].

Usually, the oxidation kinetic process of steel can be described by the equation of: [32]

$$\Delta W^2 = kt \tag{2}$$

where, ΔW is the mass gain per unit area in mg/cm^2, k is the oxidation rate constant in mg^2/(cm^4·min), and t is the reaction time in min. It is equal to another formula with an explicit analytic expression [33–39]:

$$\alpha = \frac{\Delta V}{V_0} = \frac{1}{L^0}\sqrt{\frac{t}{t_\Phi}} \tag{3}$$

$$t_\Phi = \frac{\upsilon_m}{D(C - C^{eq})} = \frac{\upsilon_m}{D_0(C - C^{eq})}\exp\left(\frac{\Delta E + \Delta\varepsilon}{RT}\right) \tag{4}$$

where, α is defined as the oxidation degree, V_0 is the original volume of the sample and ΔV is the volume of the oxidized part of the sample. The characteristic oxidation time, t_Φ, is introduced into Eq. (3). The value of it is inversely proportional to that of k. It is obvious that the reaction fraction α is equal to 1 when $t = t_\Phi$. D is the diffusion coefficient of the certain component, here D_0 is a constant. C and C^{eq} are the concentration of the certain ions at the interface between the alloy matrix and the oxides scale and at the outer surface of

the oxides scale in equilibrium condition, respectively. ΔE and $\Delta\varepsilon$ are the apparent activation energies of interface chemical reaction and diffusion process, respectively. The rest of parameters are related to the external physical characteristic, where υ_m is a coefficient related to the density of the substance and reaction, L_0 is the original thickness of the alloy. A is defined for convenience:

$$A = \frac{\upsilon_m}{D_0(C - C^{eq})} \tag{5}$$

If the reaction rate is determined by the diffusion of oxygen anions in the oxides scale, oxygen concentration in the substance follow Sieverts' law:

$$C = k_0\sqrt{P_{O_2}} \tag{6}$$

here, P_{O_2} is the oxygen partial pressure in the ambience, and k_0 is the Sieverts' constant depending on the temperature.

However, the Eqs. (2) and (3) only describes the reaction of a plate sample without considering the reaction progress on the edges and corners of the sample. Therefore, a deviation can be introduced to the kinetic analysis if the thickness of the sample is not far more less than the length and width of

itself. A three-dimensional model was proposed for a cuboid sample [40]:

$$\alpha = 1 - (1 - \frac{2}{L_0}\sqrt{\frac{2t}{t_\Phi}})^2 (1 - \frac{2}{H_0}\sqrt{\frac{2t}{t_\Phi}}) \quad (7)$$

where, H_0 is the thickness of the cuboid sample.

Here, the corresponding oxidation kinetic constant k_Φ can be defined as:

$$k_\Phi = 1/t_\Phi \quad (8)$$

When the oxidation of the sample is controlled by interface chemical reaction, the formula of the model is changed:

$$\alpha = 1 - (1 - \frac{2}{L_0}\frac{t}{t_{\Phi i}})^2 (1 - \frac{2}{H_0}\frac{t}{t_{\Phi i}}) \quad (9)$$

where,

$$t_{\Phi i} = \frac{\upsilon_m}{(C - C^{eq})}\exp(\frac{\Delta E}{RT}) \quad (10)$$

A_i is introduced in to the equation for convenience:

$$A_i = \frac{\upsilon_m}{(C - C^{eq})} \quad (11)$$

Here, the corresponding oxidation kinetic constant $k_{\Phi i}$ can be defined as:

$$k_{\Phi i} = 1/t_{\Phi i} \quad (12)$$

It is easy to know that

$$\frac{\Delta m}{S_0} = \frac{m_0 \gamma_{O/Cations}}{S_0}\alpha = \frac{\Delta m_{max}}{S_0}\alpha \quad (13)$$

Here, m_0 is the mass of the sample before reaction, $\gamma_{O/Cations}$ is the mass ratio of oxygen anions to cations in the oxides, Δm_{max} is the max mass gain of the sample, $t_{\Phi i}$ is the characteristic oxidation time of the interface chemical reaction controlled process. Although the latter parameter varies with the oxidation process, here it is assumed to be constant. Substituting Eq. (13) into Eq. (7) and (9), respectively, yields

$$\frac{\Delta m}{S_0} = \frac{\Delta m_{max}}{S_0}[1 - (1 - \frac{2}{L_0}\sqrt{\frac{2t}{t_\Phi}})^2 (1 - \frac{2}{H_0}\sqrt{\frac{2t}{t_\Phi}})] \quad (14)$$

$$\frac{\Delta m}{S_0} = \frac{\Delta m_{max}}{S_0}[1 - (1 - \frac{2}{L_0}\frac{t}{t_{\Phi i}})^2 (1 - \frac{2}{H_0}\frac{t}{t_{\Phi i}})] \quad (15)$$

Eqs. (14) and (15) were employed for the kinetic analysis of the experimental results. The fitting results are shown in Fig. 4. The values of the characteristic oxidation time in the adopted models can be referred from Fig. 5. The oxidation process of DX51D + Z steel sample is kinetically determined by interface chemical reaction. It is because of the relatively low oxidation resistance of the oxides scale on its surface. The oxidation processes of the other steel samples at higher temperatures are chemical reaction rate controlled. On the contrary, the reaction at lower temperatures are always rate

determined by diffusion step. It is clear to be observed that the mass gain does not linearly change with exposure time, even the reaction rate determine step is chemical reaction. It is the difference between the oxidation kinetics of cuboid and plate: A parabolic mass gain curve for both plate and cuboid imply that the reaction is diffusion controlled, but the mass gain curve of a chemical reaction-controlled cuboid reaction can be non-linear.

Table 2 gives the fitted parameters in the models for the oxidation process. The activation energy for diffusion step controlling reactions varies from 344.3 kJ/mol to 602.9 kJ/mol. The 50WW800 steel samples with the highest value was oxidized the slowest. The apparent activation energies for the interface chemical reaction step controlling reactions are less than100 kJ/mol. The values for the DX51D + Z and 30Q140 steel sample are the more reliable because the calculation employs at least three data points. For the two samples, the apparent activation energies are 55.2 ± 6.8 kJ/mol and 57.7 ± 16.9 kJ/mol. The definitions of characteristic oxidation time imply that the values of D0 and $\Delta\varepsilon$ can be calculated out for all the samples except for DX51D + Z. However, it should be noted that the two values cannot be obtained from the current kinetic data. The reason is that the chemical composition and structure of the oxides scale vary a lot when the oxidation kinetic mechanism changes [41,42]. The oxides products become porous and coarse with the development of the oxides composition in change from the diffusion controlling kinetic region to the interface chemical reaction controlling kinetic region. It means, the diffusion coefficient is not the one for the ions crossing the diffusion barrier which composed by Si and Al based oxides anymore.

In addition, the corresponding reaction kinetic constants of the four types of commencial steels were calculated based on the adopted models according to Eqs. (8) and (12). As the results shown in Fig. 6, it is indicate that the automotive steel (DX51D + Z) with low contents of Si and Al alloy elements could be oxidized rapidly at relative low temperature, of which the oxidation reaction kinetic constant is above 1.3×10^{-7} when the reaction temperature higher than 1030 °C. As for silicon steel with relative high contents of Si or Al, the oxidation rate is very slow at low temperature (<1130 °C). It should be ascribed that Si and Al would form an oxidation protection layer, which will retard the formation of oxidation layer on the surface of steel. The oxidation rate begin to increasing above 1130 °C due to the formed oxidation protection layer become porous at high temperature [43]. Moreover, compared to non-oriented silicon steel (50WW800 and 50WW470), the oriented silicon steel (30Q140) containing more silicon and less aluminum. The reaction rate of non-oriented silicon steel is higher than that of oriented silicon steel because the protection layer based on aluminum oxide is denser than that of silicide [15].

There is another parameter (Δm_{max}) to evaluate the thicknees obtaiend oxdie scales in different temperatures. In the view of thermodynamic, it can be calculated from the composition of the sample. For instance, Δm_{max} of a pure iron would be 42.86 mass% of the initial mass of the sample in pure oxygen atmosphere. With the assumption that the max mass gain of a certain sample keeps the same at different reaction temperatures, the value of Δm_{max} was predicted by Eq. (15). The predicted value was then substituted into Eq. (14) in the
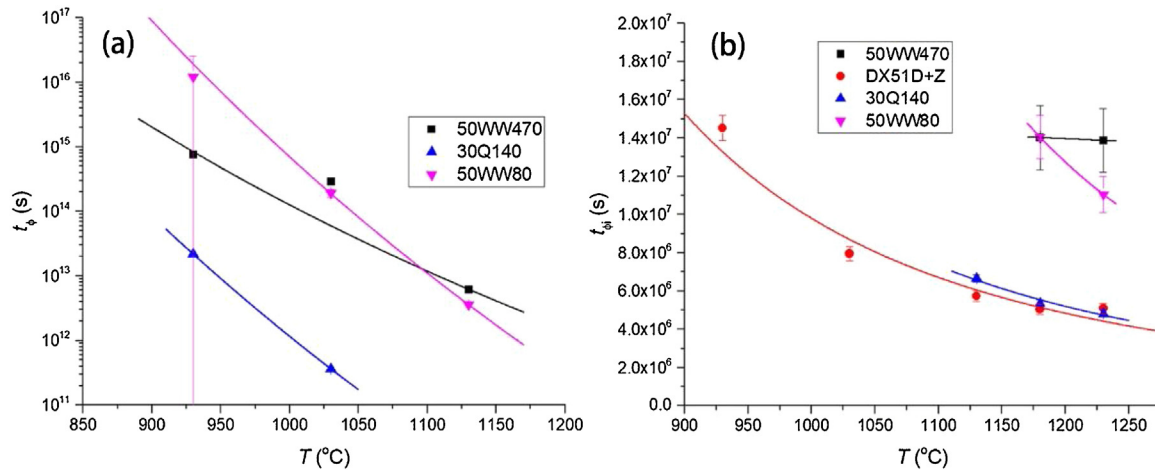
Fig. 5 – The characteristic time in the kinetic model described by (a) Eq. (14); and (b) Eq. (15).

Table 2 – Kinetic parameters for the oxidation of steel samples.

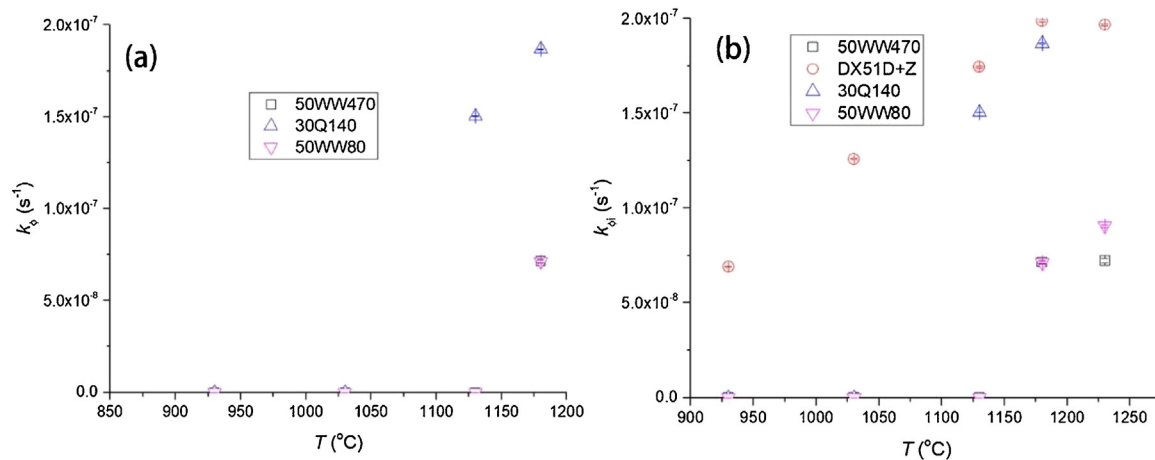| Sample		chem			diff		
		Value	Error			Value	Error
50WW470	A_i	10131.08	73845.62	A		2.35E-07	1.20E-07
	ΔE	87404.64	91056.32	$\Delta E + \Delta \varepsilon$		581859.2	6715.561
DX51D + Z	A_i	46789.26	65044.69	A		–	–
	ΔE	57663.4	16920.72	$\Delta E + \Delta \varepsilon$		–	–
30Q140	A_i	53192.13	32146.87	A		1.26E-07	1.11E-06
	ΔE	55205.48	6846.15	$\Delta E + \Delta \varepsilon$		517618.7	102403.9
50WW800	A_i	1.01E+07	1.04E+08	A		3.56E-08	6.38E-07
	ΔE	3940.393	126724.8	$\Delta E + \Delta \varepsilon$		597546	237086.9

Fig. 6 – The reaction kinetic constants in the kinetic model described by (a) Eq. (8) (b) Eq. (12).

modeling procedure. Eq. (14) was not be employed for the prediction of the value of Δm_{max}. The reason is that the fitting quality of Eq. (14) was not sensitive to the value of Δm_{max}. As a result, the value of Δm_{max} can be used to evaluate how serious would be oxidation be in the interface chemical reaction rate-determining oxidation process.

It is suspected that the value of Δm_{max} could be affected by the alloy contents of the alloy. Fig. 7 indicates the effects of Si and Al contents in the steel on the value of Δm_{max}. It shows that the Al content in the steel can have strong influence on this predicted value. Combining the former result from Eq. (1), it is noted that although the oxidation resistance of the steel samples were mostly contributed by Al other than Si for the diffusion rate determining oxidation, but Al has negative contribution on the oxidation degree of the sample for the interface chemical reaction rate determining oxidation.
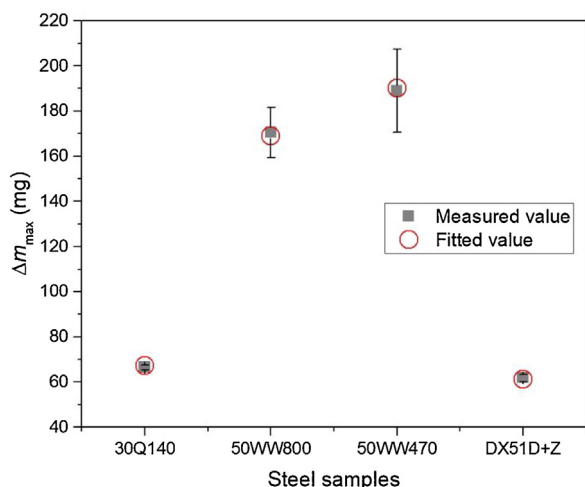
Fig. 7 – The predicted max mass gain of the steel samples with different contents of Al and Si.

3.4. Explore preheating temperature for different steel

During the hot rolling process, preheating is one of most important steps. The obtained bulk steel is preheated to sufficient high temperature can not only reduce the strength of slab, but also form enough thickness of oxide scale on the surface of slab to remove the surface defect and inclusion of the slab, which is beneficial for improving the surface quality of the obtained slab. However, with the developing demand on the saving energy, it is necessary to lower the preheating temperature as much as possible. Hence, we have to explore the lowest preheating temperature for different types of steel to satisfy the demand of strength for rolling and thickness of oxide scale.

Based on the aforementioned oxidation kinetic analysis, it is known that the reaction kinetic constants of automotive steel, oriented silicon steel and non-oriented silicon steel changed obviously at 1030 °C, 1130 °C and 1180 °C, respectively. Hence, when the preheating duration is controlled for the same time in the real hot rolling process, in order to obtain enough thickness of oxide scale, the lowest preheating temperature of different types steel range from high to low should be non-oriented silicon steel (1180 °C), oriented silicon steel (1130 °C) and automotive steel (1030°). Considering the principal differences of the contents of Si and Al in these samples, it is reasonable to speculate that the lowest preheating temperature for commercial steel with low content of Si and Al should be 1030 °C, for the steel with high content of Si and low content of Al should be 1130 °C, for the steel with high content of Al should be 1180 °C. These results are important reference parameter for different commercial steel in the real hot rolling produciton.

4. Conclusions

1) The oxidation resistance of commercial steel samples with different Al and Si content were investigated experimentally. The results indicate that Al provide stronger diffusion resistance than Si in the diffusion-controlling oxidation region. However, high content of Al in these steel samples resulted in higher predicted max mass gain in the oxidation.

2) Both Al and Si based oxides form at the steel-oxides interface as diffusion barrier. Whilst, low concentration of alloy elements in automotive steel (DX51D + Z) cannot provide efficient diffusion resistance. Outward diffusion of cations in oriented silicon steel (30Q140) with relatively high concentration of alloy elements resulted in porous metallic layer under the oxide scale.

3) A three-dimensional oxidation kinetic model was introduced for the cuboid samples. The activation energies of the oxidation processes were calculated via the model. As typical values, the activation energy of diffusion controlling oxidation of non-oriented silicon steel (50WW800) is 602.9 ± 231.7 kJ/mol, and the activation energy of interface chemical reaction controlling oxidation of automotive steel (DX51D + Z) is 55.2 ± 6.9 kJ/mol.

4) When the preheating duration is controlled for the same time in the real hot rolling process, in order to obtain enough thickness of oxide scale, the lowest preheating temperature of different types steel range from high to low should be the steel with high content of Al (1180 °C), the steel with high content of Si and low content of Al (1130 °C) and the steel with high contents of Si and Al (1030 °C).

Conflicts of interest

The authors declare no conflicts of interest.

Acknowledgement

REFERENCES

[1] Noh W, Lee JM, Kim DJ, Song JH, Lee JMG. Effects of the residual stress, interfacial roughness and scale thickness on the spallation of oxide scale grown on hot rolled steel sheet. Mater Sci Eng A 2019;739:301–16, http://dx.doi.org/10.1016/j.msea.2018.10.009.

[2] Cahn RW. Fe (Iron) Binary Alloy Phase Diagrams. Alloy Phase Diagrams, vol. 3. ASM International; 2016. p. 340–61, http://dx.doi.org/10.31399/asm.hb.v03.a0006162.

[3] Shahsanaei M, Pour-Ali S, Kiani-Rashid AR, Virtanen S. Carbide fragmentation and dissolution in a high-carbon high-chromium steel using hot rolling process: microstructure evolution, wear, high-temperature oxidation, and chloride-induced corrosion properties. CORROSION 2018;74:958–70, http://dx.doi.org/10.5006/2749.

[4] Chandra-ambhorn S, Phadungwong T, Sirivedin K. Effects of carbon and coiling temperature on the adhesion of thermal oxide scales to hot-rolled carbon steels. Corros Sci 2017;115:30–40, http://dx.doi.org/10.1016/j.corsci.2016.11.014.

[5] Yu XL, Jiang ZY, Zhao JW, Bin Wei D, Zhou CL. Effect of cooling rate on oxidation behaviour of microalloyed steel. Appl Mech Mater 2013;395–396:273–8, http://dx.doi.org/10.4028/www.scientific.net/AMM.395-396.273.

[6] Yu X, Jiang Z, Zhao J, Wei D, Zhou C, Huang Q. Effect of a grain-refined microalloyed steel substrate on the formation mechanism of a tight oxide scale. Corros Sci 2014;85:115–25, http://dx.doi.org/10.1016/j.corsci.2014.04.006.

[7] Yu X, Jiang Z, Zhao J, Wei D, Zhou C, Huang Q. Microstructure and microtexture evolutions of deformed oxide layers on a hot-rolled microalloyed steel. Corros Sci 2015;90:140–52, http://dx.doi.org/10.1016/j.corsci.2014.10.005.

[8] Yu X, Jiang Z, Wang X, Wei D, Yang Q. Effect of coiling temperature on oxide scale of hot-rolled strip. Adv. Mater. Res 2012;415–417:853–8, http://dx.doi.org/10.4028/www.scientific.net/AMR.415-417.853.

[9] Cao G, Li Z, Tang J, Sun X, Liu Z. Oxidation kinetics and spallation model of oxide scale during cooling process of low carbon microalloyed steel. High Temp Mater Process 2017;36:927–35, http://dx.doi.org/10.1515/htmp-2015-0248.

[10] Yearian HJ, Randell EC, Longo TA. The structure of oxide scales on chromium steels. CORROSION 1956;12:55–65, http://dx.doi.org/10.5006/0010-9312-12.10.55.

[11] Taniguchi S, Furukawa T, Shibata T. Effects of Cu and other tramp elements on steel properties. Failure of scales formed on Cu-containing low carbon steels during cooling. ISIJ Int 1997;37:263–71, http://dx.doi.org/10.2355/isijinternational.37.263.

[12] Suarez L, Schneider J, Houbaert Y. Effect of Si on high-temperature oxidation of steel during hot rolling. Defect Diffus Forum 2008;273–276:655–60, http://dx.doi.org/10.4028/www.scientific.net/DDF.273-276.655.

[13] Fukagawa T, Okada H, Maehara Y. Mechanism of red scale defect formation in Si-added hot-rolled steel sheets. ISIJ Int 1994, http://dx.doi.org/10.2355/isijinternational.34.906.

[14] Okada H, Fukagawa T, Ishihara H, Okamoto A, Azuma M, Matsuda Y. Prevention of red scale formation during hot rolling of steels. ISIJ Int 1995, http://dx.doi.org/10.2355/isijinternational.35.886.

[15] Cheng WJ, Wang CJ. High-temperature oxidation behavior of hot-dipped aluminide mild steel with various silicon contents. Appl Surf Sci 2013;274:258–65, http://dx.doi.org/10.1016/j.apsusc.2013.03.030.

[16] Alaoui Mouayd A, Koltsov A, Sutter E, Tribollet B. Effect of silicon content in steel and oxidation temperature on scale growth and morphology. Mater Chem Phys 2014, http://dx.doi.org/10.1016/j.matchemphys.2013.10.037.

[17] Liu XJ, He YQ, Cao GM, Jia T, Wu TZ, Liu ZY. Effect of Si content and temperature on oxidation resistance of Fe-Si alloys. J Iron Steel Res Int 2015, http://dx.doi.org/10.1016/S1006-706X(15)60036-X.

[18] Yuan Q, Xu G, xing Zhou M, He B. New insights into the effects of silicon content on the oxidation process in silicon-containing steels. Int J Miner Metall Mater 2016, http://dx.doi.org/10.1007/s12613-016-1322-0.

[19] Chen RY, Yuen WYD. Review of the high-temperature oxidation of iron and carbon steels in air or oxygen. Oxid Met 2003;59:433–68, http://dx.doi.org/10.1023/A:1023685905159.

[20] Su Y, Zhang S, Fu G, Liu Q, Tang Y. High-temperature oxidation behavior of Fe-Si-Ce alloys. High Temp Mater Process 2016;35:177–83, http://dx.doi.org/10.1515/htmp-2014-0171.

[21] Dunning JS, Alman DE, Rawers JC. Influence of silicon and aluminum additions on the oxidation resistance of a lean-chromium stainless steel. Oxid Met 2002, http://dx.doi.org/10.1023/A:1015344220073.

[22] Delaunay D, Huntz AM, Lacombe P. Impurities influence on oxidation kinetics of Fe-Ni-Cr-Al alloys. Corros Sci 1984;24:13–25, http://dx.doi.org/10.1016/0010-938X(84)90132-X.

[23] Kumar A, Douglass DL. Modification of the oxidation behavior of high-purity austenitic Fe-14Cr-14Ni by the addition of silicon. Oxid Met 1976;10:1–22, http://dx.doi.org/10.1007/BF00611695.

[24] Martínez-Cázares GM, Mercado-Solís RD, Colás R, Garza-Montes-de-Oca NF. High temperature oxidation of silicon and copper–silicon containing steels. Ironmak Steelmak 2013;40:221–30, http://dx.doi.org/10.1179/1743281212Y.0000000064.

[25] Chang Y-N. Roles of silicon and aluminium in pickling behaviour of low alloy hot rolled steel. Br Corros J 1994;29:136–9, http://dx.doi.org/10.1179/000705994798267818.

[26] Chang YN, Wei FI. High temperature oxidation of low alloy steels. J Mater Sci 1989;24:14–22, http://dx.doi.org/10.1007/BF00660927.

[27] Ecer GM, Meier GH. Oxidation of high-chromium Ni-Cr alloys. Oxid Met 1979;13:119–58, http://dx.doi.org/10.1007/BF00611976.

[28] Tung HM, Stubbins JF. Incipient oxidation kinetics and residual stress of the oxide scale grown on Haynes 230 at high temperatures. Mater Sci Eng A 2012;538:1–6, http://dx.doi.org/10.1016/j.msea.2011.10.114.

[29] Basabe VV, Szpunar JA. Growth rate and phase composition of oxide scales during hot rolling of low carbon steel. ISIJ Int 2004;44:1554–9, http://dx.doi.org/10.2355/isijinternational.44.1554.

[30] Ecer GM, Singh RB, Meier GH. The influence of superficially applied oxide powders on the high-temperature oxidation behavior of Cr2O3-forming alloys. Oxid Met 1982;18:55–81, http://dx.doi.org/10.1007/BF00656095.

[31] Chen ZY, Wang LJ, Li FS, Chou KC. Oxidation mechanism of Fe-16Cr alloy as SOFC interconnect in dry/wet air. J Alloys Compd 2013;574:437–42, http://dx.doi.org/10.1016/j.jallcom.2013.05.072.

[32] Wang CJ, Chen SM. The high-temperature oxidation behavior of hot-dipping Al-Si coating on low carbon steel. Surf Coatings Technol 2006;200:6601–5, http://dx.doi.org/10.1016/j.surfcoat.2005.11.031.

[33] Chou KC, Li Q, Lin Q, Jiang LJ, K Di Xu. Kinetics of absorption and desorption of hydrogen in alloy powder. Int J Hydrogen Energy 2005;30:301–9, http://dx.doi.org/10.1016/j.ijhydene.2004.04.006.

[34] Chou K-C. A kinetic model for oxidation of Si-Al-O-N materials. J Am Ceram Soc 2006;89:1568–76, http://dx.doi.org/10.1111/j.1551-2916.2006.00959.x.

[35] Chou KC, Xu K. A new model for hydriding and dehydriding reactions in intermetallics. Intermetallics 2007;15:767–77, http://dx.doi.org/10.1016/j.intermet.2006.10.004.

[36] Hou X, Chou KC, Zhong X, Seetharaman S. Oxidation kinetics of aluminum nitride at different oxidizing atmosphere. J Alloys Compd 2008;465:90–6, http://dx.doi.org/10.1016/j.jallcom.2007.10.066.

[37] Hou XM, Chou KC, Hu XJ, Zhao HL. A new measurement and treatment for kinetics of isothermal oxidation of Si3N4. J Alloys Compd 2008;459:123–9, http://dx.doi.org/10.1016/j.jallcom.2007.04.255.

[38] Hou XM, Chou KC. Quantitative interpretation of the parabolic and nonparabolic oxidation behavior of nitride ceramic. J Eur Ceram Soc 2009;29:517–23, http://dx.doi.org/10.1016/j.jeurceramsoc.2008.06.015.

[39] Hou XM, Chou KC, Zhang M. The model for oxidation kinetics of titanium nitride coatings. Int J Appl Ceram Technol 2010;7:248–55, http://dx.doi.org/10.1111/j.1744-7402.2008.02342.x.

[40] Chou KC, Hou XM. Kinetics of high-temperature oxidation of inorganic nonmetallic materials. J Am Ceram Soc

2009;92:585–94,
http://dx.doi.org/10.1111/j.1551-2916.2008.02903.x.

[41] Chen Z, Wang L, Li F, Chou KC, Sun Z. The effects of temperature and oxygen pressure on the initial oxidation of stainless steel 441. Int J Hydrogen Energy 2014;39:10303–12, http://dx.doi.org/10.1016/j.ijhydene.2014.04.188.

[42] Chen Z, Wang L, Li F, Chou K. Thermodynamic analysis of the corrosion of Fe-16Cr alloy interconnect of solid oxide fuel cell under various atmospheres. High Temp Mater Process 2014;33:439–45, http://dx.doi.org/10.1515/htmp-2013-0104.

[43] Nová KP, Nová K. Oxidation behavior of Fe–Al, Fe–Si and Fe–Al–Si intermetallics. Materials (Basel) 2019;12:1748, http://dx.doi.org/10.3390/ma12111748.